CERN-ACC-NOTE-2022-0021

August 2022

Report from LHC MD 3312: Replicating HL-LHC DA

J. Dilly, M. Albert, F. Carlier, J. Coello de Portugal, B. Dalena, E. Fol, M. Hofer, E.H. Maclean, L. Malina, T. Persson, M. Solfaroli Camillocci, M. Spitznagel, R. Tomás, A. G.-T. Valdivieso

Keywords: HL-LHC, dynamic aperture, amplitude detuning, ats

Summary

During MD3312 on the 30.10.2018 the non-linear conditions in the insertion regions of the planned HL-LHC were replicated to our best knowledge and within the capabilities of the hardware currently available in the LHC: A flat ATS-optics scheme of $\beta^* = 15\,\mathrm{cm}/60\,\mathrm{cm}$ in IP1 and IP5 was applied as well as sextupole, octupole and (normal) dodecapole errors were introduced into the machine via the corrector magnets in the interaction regions. Amplitude detuning and dynamic aperture measurements were performed at different working points. A first analysis, based on beam lifetime observations, is given in this note. Two initial challenges, namely an increase in β-beating due to the tune-feedback not being adapted to the ATS-scheme as well as the correction of a waist-shift in IP5, are also presented.

Contents

1 Motivation and procedure overview

In July 2017, MD2158 [1] was performed to explore the prospects for the High Luminosity (HL) - LHC linear and non-linear optics commissioning by enhancing sextupole and dodecapole sources in the ATLAS and CMS interaction regions (IR). While overall the MD was successful, measurements during that MD suffered from the loss of AC-Dipole adiabaticity [2, 3] under the influence of the strong skew sextupoles (a_3) in the IR. In consequence, this lead to dramatic blow-up of the beam after - even small - AC-Dipole kicks. Furthermore, following studies of the influence of strong dodecapole errors (b_6) were complicated by the blown up beam. Questions were raised on how this effect will limit the ability to perform linear optics commissioning [4, 5] in the HL-LHC, taking into account the strong nonlinear errors anticipated at low-β^* [6, 7, 8, 9].

Low β^* is provided by using flat-optics with $\beta^* = 60\,\text{cm}/15\,\text{cm}$, which may be used in the HL-LHC as well [6, 10, 11]. Using this configuration also allows to follow up on the results from the flat-optics MD program (MD2148) [12, 13]. After checking for residual coupling in the machine, the initial part of MD3312 was thus dedicated to re-visit linear optics corrections in the flat-ATS scheme. In particular, the waist of the β-function in interaction point (IP) 5, was shifted to correct β^*, which has been tested by luminosity scans and K-modulation procedures [14].

Procedure

High-order errors were artificially introduced with the MCOX, MCOSX, MCSX, MCSSX and MCTX in IR1 and IR5 [15]. Beam 1 has been used to study amplitude detuning throughout the MD, while dynamic aperture (DA) measurements were performed on Beam 2. For the amplitude detuning study vertical and horizontal kicks were executed independently, kicking only lightly in the respective opposite plane to observe coupling effects. The DA measurements on the other hand were performed by diagonal kicks at different working points of the tunes. Goal of the DA measurements was to observe the impact of strong nonlinear errors in the low-beta IRs on the DA of forced oscillations [16], not only to quantify the expected limits during HL-LHC linear optics commissioning mentioned above, but also to allow benchmarking of DA simulations. Both studies were executed at different tune settings, i.e. working points in the tune diagram (see Figs. 14 and 17), to probe the influence of various resonances.

To avoid blow-up and distortion of the beam by the influence of the lower orders, especially at high kick amplitudes, as seen in the past, the individual influence of b_6 has been studied first. After successful measurements, b_4, a_3, b_3 and a_4 were trimmed in as well, and further amplitude detuning and DA kicks were conducted.

Unfortunately, instead of probing close to the diagonal resonances as before (working point 3 in Fig. 17a), we kicked accidentally almost directly on the $-4Q_x + Q_y$ resonance (working point 3 in Fig. 17b), a dodecapole resonance. With all correctors powered, the beams were dumped due to too high losses during the first excitation, and could not be refilled due to time constraints. For this reason, studies with crossing angles to measure feed-down, as described in the MD request [17], could not be conducted.

Nonetheless, measurements during MD3312 generated a plethora of data, revealing crucial insights into the physics of HL-LHC beam optics as shown in the following chapters.

Table 1: MD Time-line (Part 1). Key measurements are shown in **bold**.

12:00→13:50	MD Setup. Get machine to end-of-squeeze, flat-optics, 6.5TeV.
13:50→14:05	Coupling Measurements: Beam 1: $-2 \cdot 10^{-4} + 12 \cdot 10^{-4} i$ Beam 2: $-14 \cdot 10^{-4} + 6 \cdot 10^{-4} i$
14:05→14:15	**K-Modulation:** IP5, 5A right: 14:07:10→14:09:50 left: 14:09:50→14:12:29
14:15→14:44	**Trim waist-shift** for β^* correction. Trim: *LHCBEAM/2018_global_ats_flat_b1_for_ip5_waist* Stepwise 0% to 80%.
14:44→14:50	**K-Modulation:** IP5, 5A right: 14:44:00→14:46:30 left: 14:46:40→14:49:20
14:30→14:50	**β-beating measurements.** Beam 1 kickgroup: *b1_after_betastar_corr* Beam 2 kickgroup: *b2_afterbetastarcorr*
14:55→15:02	**Trimming RCTX**, 60A Trim: *LHCBEAM/2018_MD4_replicatingHL_b6* to 1.0
Beam 1	Amplitude Detuning
15:07	Working point at: $Q_{x,y}$: 0.283, 0.31 $Q_{x.y}^{ACD}$: 0.271, 0.325
15:07→15:23	**Vertical kicks for amplitude detuning.** (10% horizontal) Kickgroup: *b1_for_amplitude_detuning_vertical*
15:23→15:30	**Horizontal kicks for amplitude detuning.** (10% vertical) Kickgroup: *b1_for_amplitude_detuning_horizontal*
15:45	Moving working point to: $Q_{x,y}$: 0.283, 0.31 $Q_{x.y}^{ACD}$: 0.275, 0.30
15:45→15:45	**Vertical kick for amplitude detuning.** (10% horizontal) *One kick only!* Kickgroup: *b1_for_amplitude_detuning_vertical_newwp*
Beam 2	Dynamic Aperture
15:10→15:20	**DA measurements.** Kickgroup: *Beam2_after_b6* $Q_{x,y}$: 0.28, 0.31 $Q_{x.y}^{ACD}$: 0.272, 0.32
15:25→15:40	**DA measurements.** Kickgroup: *Beam2_after_b6_inverted_QyDelta* $Q_{x,y}$: 0.28, 0.31 $Q_{x.y}^{ACD}$: 0.272, 0.30
15:40→15:55	**DA measurements.** Kickgroup: *Beam2_after_b6_CouplingWorkingPoint* $Q_{x,y}$: 0.28, 0.31 $Q_{x.y}^{ACD}$: 0.292, 0.30
15:55→16:05	**DA measurements.** Kickgroup: *Beam2_after_b6_OriginalWorkingPoint* $Q_{x,y}$: 0.28, 0.31 $Q_{x.y}^{ACD}$: 0.272, 0.32

Table 2: MD Time-line (Part2). Key measurements are shown in **bold**.

16:15→16:20	**Trimming RCOX**
	Trim: *LHCBEAM/2018_MD4_replicatingHL_b4* to -0.74
16:20→17:00	**Trimming RCSSX, RCSX, RCSOX**
	Trim: *LHCBEAM/2018_MD4_replicatingHL_a3* to 0.85
	Trim: *LHCBEAM/2018_MD4_replicatingHL_b3* to 1.0
	Trim: *LHCBEAM/2018_MD4_replicatingHL_a4* to 1.0
17:00→17:03	Wirescans, average emittance:
	Beam 1 *x:* 4.04 µm, *y:* 3.89 µm
	Beam 2 *x:* 2.55 µm, *y:* 4.39 µm
Beam 1	Amplitude Detuning
17:14	Working point:
	$Q_{x,y}$: 0.283, 0.31
	$Q_{x.y}^{ACD}$: 0.271, 0.325
17:14→17:30	**Vertical kick for amplitude detuning.** (1% horizontal)
	Kickgroup: *b1_for_amplitude_detuning_allcor_vertical*
Beam 2	Dynamic Aperture
17:14→17:22	**DA measurements.**
	Kickgroup: *Beam2_after_ALL_Correctors*
	$Q_{x,y}$: 0.274, 0.31
	$Q_{x.y}^{ACD}$: 0.266, 0.30
17:14→17:22	**DA measurements.** *One kick only!*
	Kickgroup: *Beam2_after_ALL_Correctors_OriginalWorkingPoint*
	$Q_{x,y}$: 0.274, 0.31
	$Q_{x.y}^{ACD}$: 0.266, 0.32
17:29→17:30	**DA measurements.** *One kick* → **dump**!
	Kickgroup: *Beam2_after_ALL_Correctors_CouplingWorkingPoint*
	$Q_{x,y}$: 0.274, 0.31
	$Q_{x.y}^{ACD}$: 0.286, 0.32

2 Measurement Summary

2.1 Full Procedure

A detailed timeline of the MD procedure is provided by Tables 1 and 2. Definitions of knobs mentioned there can be found in Appendix A. Key parameters of the MD are summarized in Table 3.

2.2 Results

2.2.1 Influence of Tune-Feedback on ATS-Optics

The machine was set up with the same optics as during MD2148, apart from the separation bumps, which were zero during MD2148. The β-beating was then measured while at the

Table 3: Key MD parameters.

Objective:	Replication of HL-LHC Dynamic Aperture and Amplitude Detuning.
MD #:	3312
Operators:	Markus Albert, Matteo Solfaroli Camillocci
Fill #:	7391
Beam Process:	MD → SQUEEZE-6.5TeV-ATS-65cm-60_15cm-2017_V1_ATSFlat@526_[END]
Date:	30 . 10 . 2018
Start Time:	12 : 00
End Time:	17 : 30
Optics:	R2017aT65_A60_15C15_60A10mL300
Crossing:	No crossing
Separation:	[0.3 / 1.4 / 0.3 / -1] mm in [IP1 / IP2 / IP5 / IP8] , *Plane:* [V / V / H / H]
Offset:	No offset

same time checking for coupling. Comparison to the β-beating from MD2148 showed a difference of about 5%.

Simulations were run to check whether this deviation could arise from orbit change (Figs. 1 and 2). Yet, these could not explain the observed difference (Figs. 3 and 4).

Intensive investigations exposed powering differences of the MQTs [18], regulated by the tune-feedback [19, 20] (see Tables 4 and 5). Further simulations concluded that the ATS optics [21] are susceptible to these changes (Figs. 5 and 6), due to the larger β-functions in the ATS arcs and the shift in phase advance between MQTs from the 90° phase advance in the non-ATS configuration, which minimizes the generated β-beating. The seen β-beating difference in Beam 1 can be fully explained by the powering change as seen in Fig. 7. In Beam 2, as shown in Fig. 8, the agreement is not as good as for Beam 1, yet this can be attributed to the change in beating being small here and a noisy measurement.

These findings have been presented at the LHC Machine Committee meeting [22]. It was concluded that a strategy was needed for the tune-feedback to take these effects for ATS-optics into account in the future, for example by excluding the MQTs in the ATS arcs from the tune feedback.

Table 4: MQT powering Beam 1. Given are the values at MD2148 in June and this MD3312 in October in Ampère, their difference and the difference in magnet strength, calculated from the powering difference. Magnets in the **ATS arcs** are shown in blue.

	Name	12-June [A]	30-October [A]	Δ [A]	ΔK [10^{-5}]
defocussing	**kqtd.a12b1**	**14.61**	**15.66**	**1.05**	**1.08**
	kqtd.a23b1	-100.58	-94.73	5.85	6.04
	kqtd.a34b1	-107.97	-102.11	5.86	6.05
	kqtd.a45b1	**-23.72**	**-22.68**	**1.04**	**1.07**
	kqtd.a56b1	**32.29**	**33.34**	**1.05**	**1.08**
	kqtd.a67b1	106.75	112.62	5.87	6.06
	kqtd.a78b1	119.84	125.68	5.84	6.03
	kqtd.a81b1	**-20.86**	**-19.81**	**1.05**	**1.08**
focussing	**kqtf.a12b1**	**-19.99**	**-14.76**	**5.23**	**5.40**
	kqtf.a23b1	-28.37	-19.72	8.65	8.93
	kqtf.a34b1	-22.52	-13.85	8.67	8.95
	kqtf.a45b1	**18.29**	**23.50**	**5.21**	**5.38**
	kqtf.a56b1	**-36.03**	**-30.81**	**5.22**	**5.39**
	kqtf.a67b1	69.76	78.43	8.67	8.95
	kqtf.a78b1	58.62	67.29	8.67	8.95
	kqtf.a81b1	**16.34**	**21.54**	**5.20**	**5.37**

Table 5: MQT powering Beam 2. Given are the values at MD2148 in June and this MD3312 in October in Ampère, their difference and the difference in magnet strength, calculated from the powering difference. Magnets in the **ATS arcs** are shown in blue.

	Name	12-June [A]	30-October [A]	Δ [A]	ΔK [10^{-5}]
defocusing	**kqtd.a12b2**	**-7.55**	**-6.96**	**0.59**	**0.61**
	kqtd.a23b2	139.05	147.61	8.56	8.84
	kqtd.a34b2	142.59	151.15	8.56	8.83
	kqtd.a45b2	**35.24**	**35.82**	**0.58**	**0.60**
	kqtd.a56b2	**-29.09**	**-28.51**	**0.58**	**0.60**
	kqtd.a67b2	-70.84	-62.28	8.56	8.83
	kqtd.a78b2	-94.61	-86.06	8.55	8.82
	kqtd.a81b2	**33.2**	**33.79**	**0.59**	**0.61**
focusing	**kqtf.a12b2**	**8.62**	**8.80**	**0.18**	**0.19**
	kqtf.a23b2	63.83	81.48	17.65	18.22
	kqtf.a34b2	58.78	76.43	17.65	18.22
	kqtf.a45b2	**-34.11**	**-33.92**	**0.19**	**0.20**
	kqtf.a56b2	**28.91**	**29.10**	**0.19**	**0.20**
	kqtf.a67b2	-34.73	-17.08	17.65	18.22
	kqtf.a78b2	-8.71	8.93	17.64	18.21
	kqtf.a81b2	**-31.31**	**-31.12**	**0.19**	**0.20**

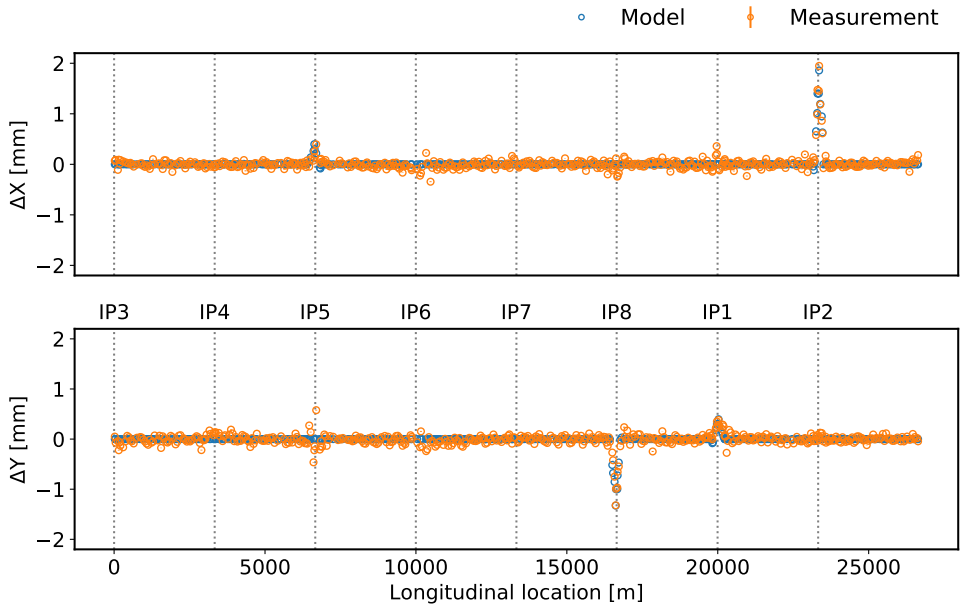

Figure 1: Orbit difference between the two MDs in Beam 1, by measurement (orange) and model via MAD-X simulation (blue).

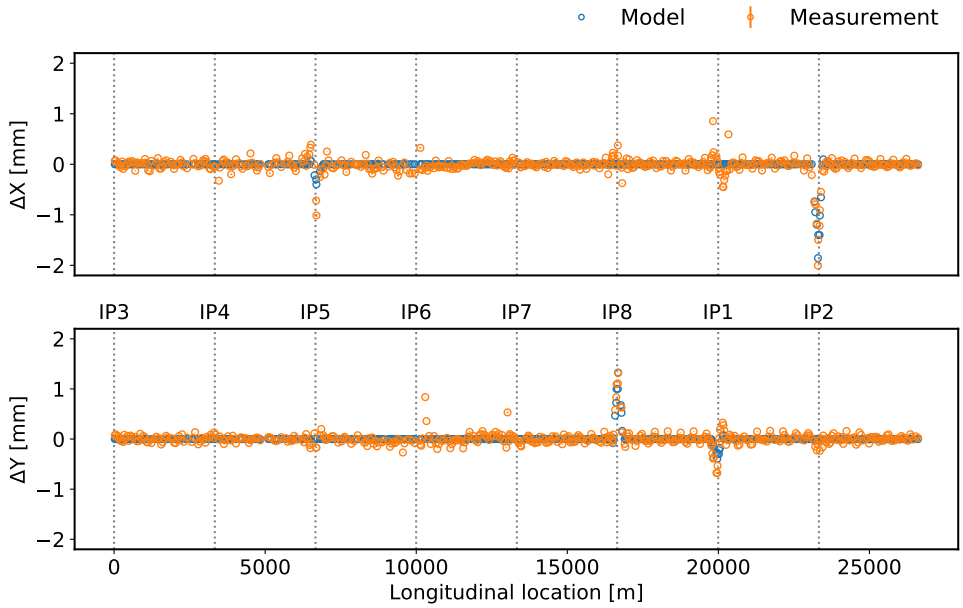

Figure 2: Orbit difference between the two MDs in Beam 2, by measurement (orange) and model via MAD-X simulation (blue).

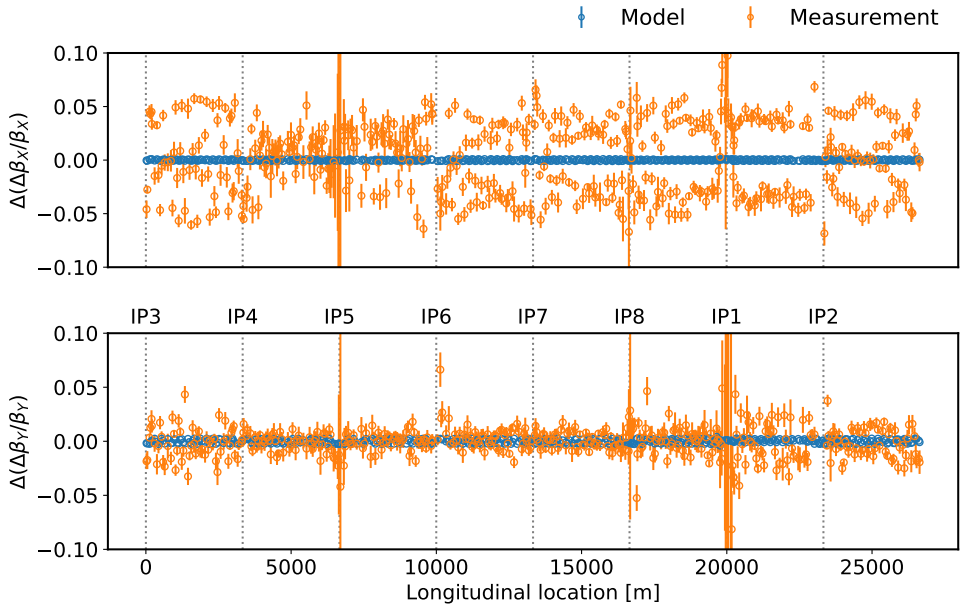

Figure 3: β-beating difference between the two MDs in Beam 1, by measurement (orange) and model via MAD-X simulation (blue).

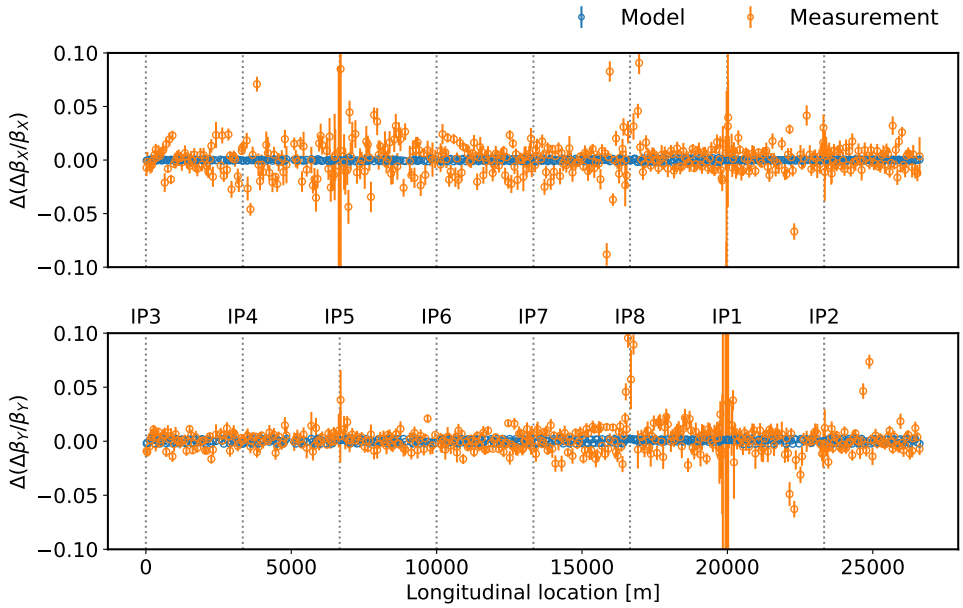

Figure 4: β-beating difference between the two MDs in Beam 2, by measurement (orange) and model via MAD-X simulation (blue).

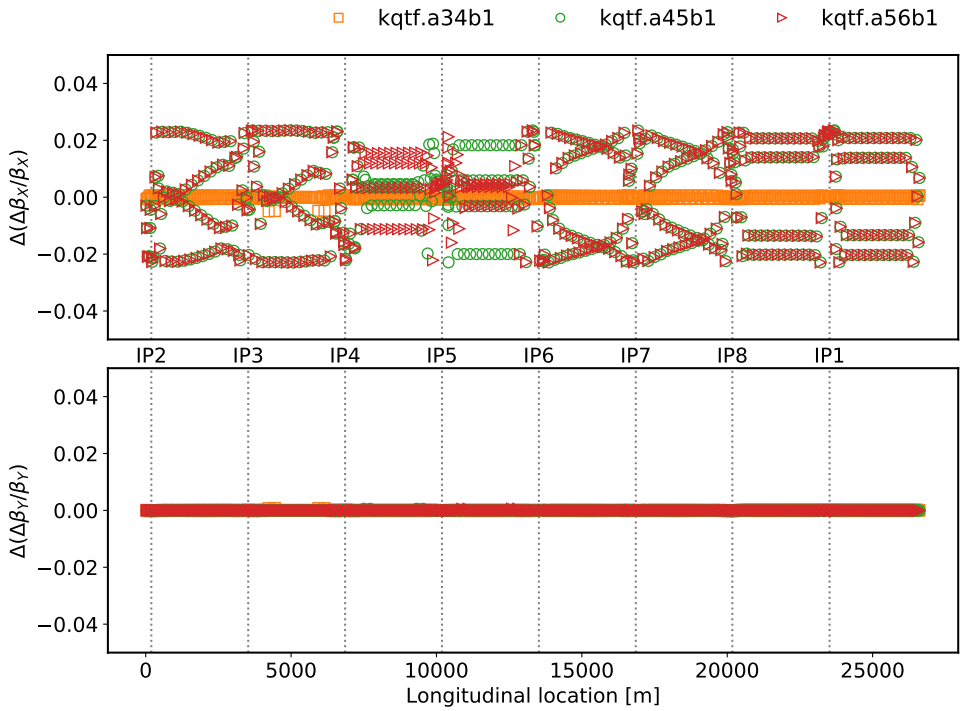

Figure 5: Simulation results of β-beating differences from ΔK values calculated in Table 4 in Beam 1. Compared are the results for **kqtf.a56b1** and **kqtf.a45b1**, which are in the ATS arcs and have both a $\Delta K \approx 5.4 \times 10^{-5}$ and **kqtf.a34b1** with $\Delta K \approx 9.0 \times 10^{-5}$. Despite the larger ΔK of the latter, its influence on β is much smaller as arc34 is not an ATS arc.

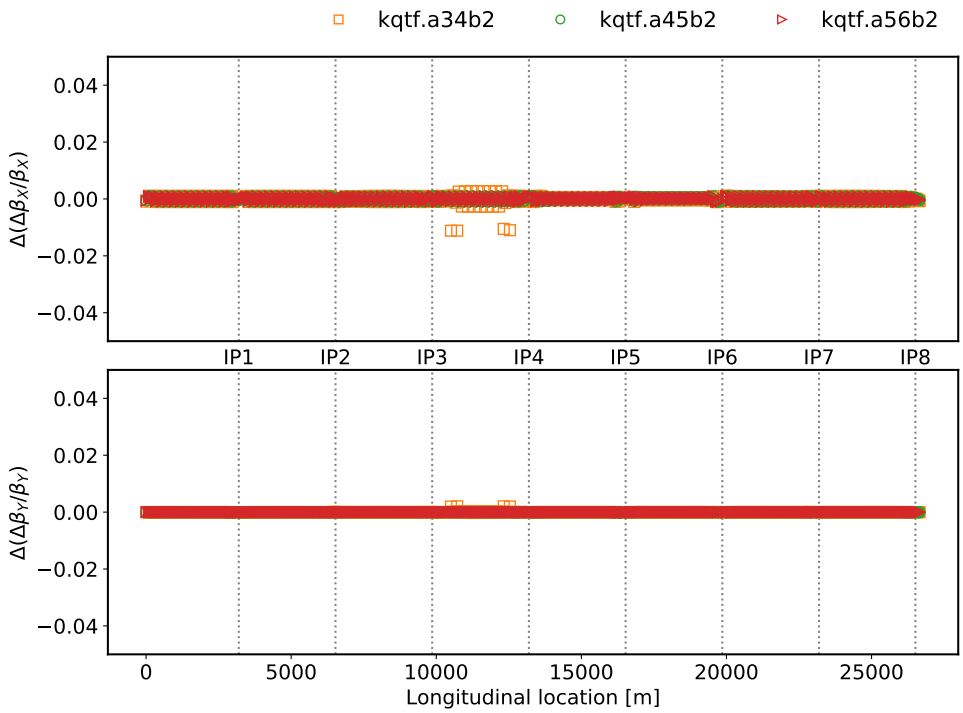

Figure 6: Simulation results of β-beating differences from ΔK values calculated in Table 5 in Beam 2. Compared are the results for **kqtf.a56b2** and **kqtf.a45b2**, which are in the ATS arcs and have both a $\Delta K = 0.2 \times 10^{-5}$ and **kqtf.a34b2** with $\Delta K \approx 18.2 \times 10^{-5}$. The influence on β of all magnets is small compared to Beam 1 (Fig. 5), as their change in K is either small, or - in the latter case - they do not lie in the ATS arcs.

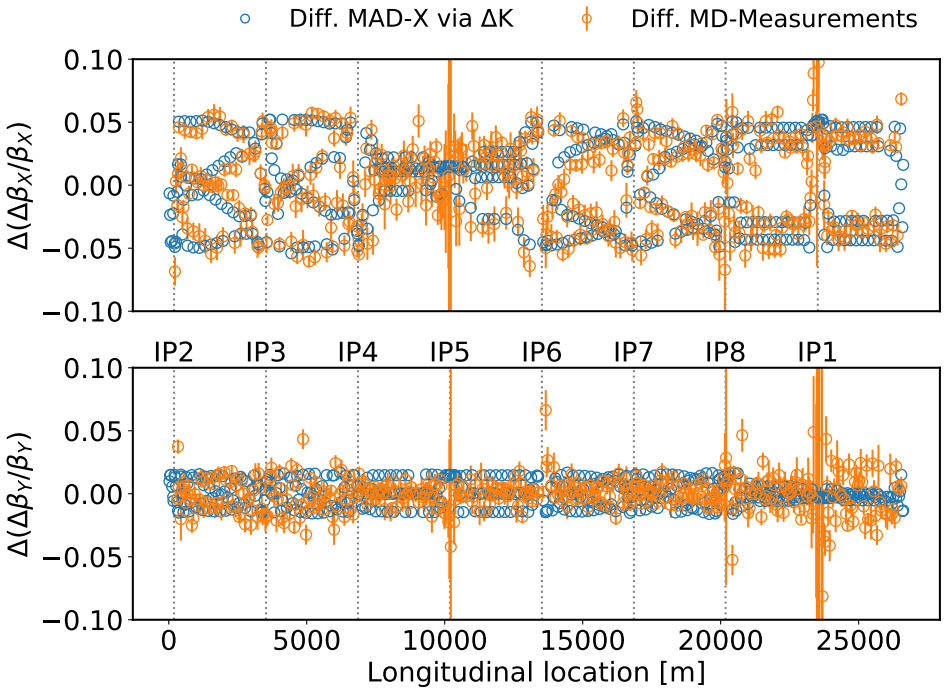

Figure 7: Comparison between the difference in Beam 1 in β-beating from MAD-X simulations from the MQT powering seen in Table 4 and the difference between the two MDs.

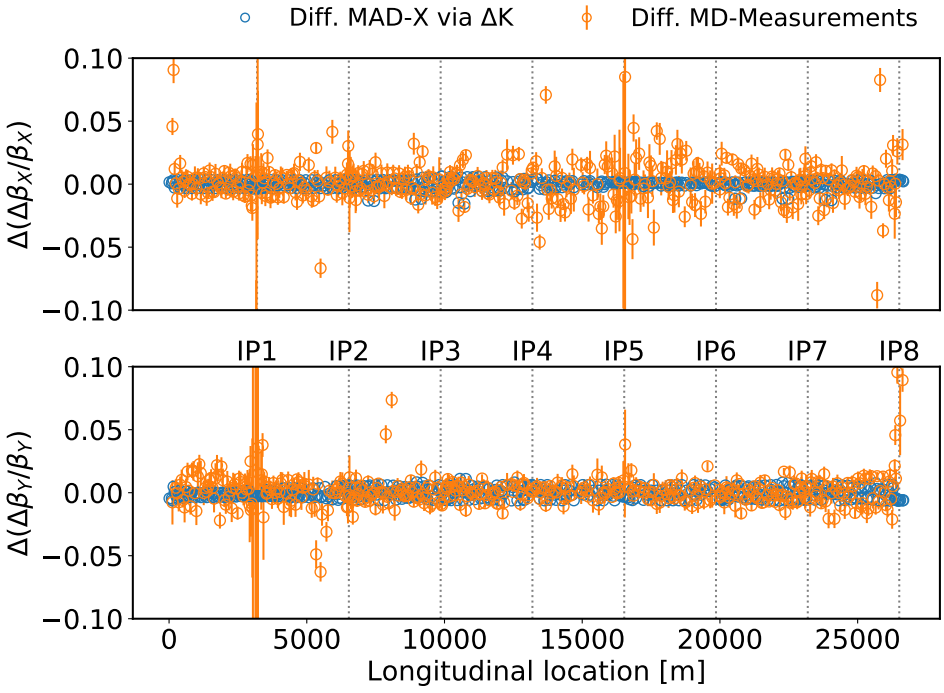

Figure 8: Comparison between the difference in Beam 2 in β-beating from MAD-X simulations from the MQT powering seen in Table 5 and the difference between the two MDs.

2.2.2 Waist correction

During the flat-optics MD2148 in June a waist shift of about -/+7 cm, in the X/Y plane respectively, was observed in Beam 1 in IP5 (see Table 6). As in June, K-modulation was performed in the present MD to check on the current status of this waist shift, which turned out to be much larger this time: Shifts between 12 cm and 26 cm were found, changing the β^* in the IP drastically (Table 6).
A correction, using the global correctors in the machine, was calculated on the fly by means of the iterative correction functionality [23] of the Beta-Beat-Gui [24]. Despite many tries, the waist shift correction was always predicted to induce some additional β-beating in the machine. As the β-beating was already 5% higher than expected (see Section 2.2.1), the correction (named *LHCBEAM/2018_global_ats_flat_b1_for_ip5_waist*, definition in Appendix A) was trimmed in stepwise and only to 80%. This corrected the waist shift successfully, as can be seen in Table 6. The increase in β-beating, dominant in the vertical plane of Beam 1, is shown in Figs. 9 and 10.

Table 6: Results from K-modulation in IP5 with 4.5 A from MD2148 and this MD, before and after trimming the global correction for the observed waist shift.

	Beam 1			
	β^* [cm]		Waist [cm]	
	X	Y	X	Y
MD2148	18.0 ± 1.2	59.6 ± 0.2	-6.7 ± 1.2	6.7 ± 1.0
MD3312 before trim	24.1 ± 1.5	69.9 ± 3.5	-11.6 ± 0.9	22.1 ± 4.5
MD3312 after trim	16.9 ± 0.5	64.0 ± 0.4	-5.2 ± 0.7	4.0 ± 2.6
	Beam 2			
	β^* [cm]		Waist [cm]	
	X	Y	X	Y
MD2148	15.3 ± 0.1	61.2 ± 0.2	1.8 ± 0.4	3.2 ± 1.1
MD3312 before trim	51.4 ± 7.2	70.7 ± 9.1	23.2 ± 2.1	-25.8 ± 9.0
MD3312 after trim	15.3 ± 0.3	61.9 ± 1.1	1.7 ± 1.0	6.6 ± 4.0

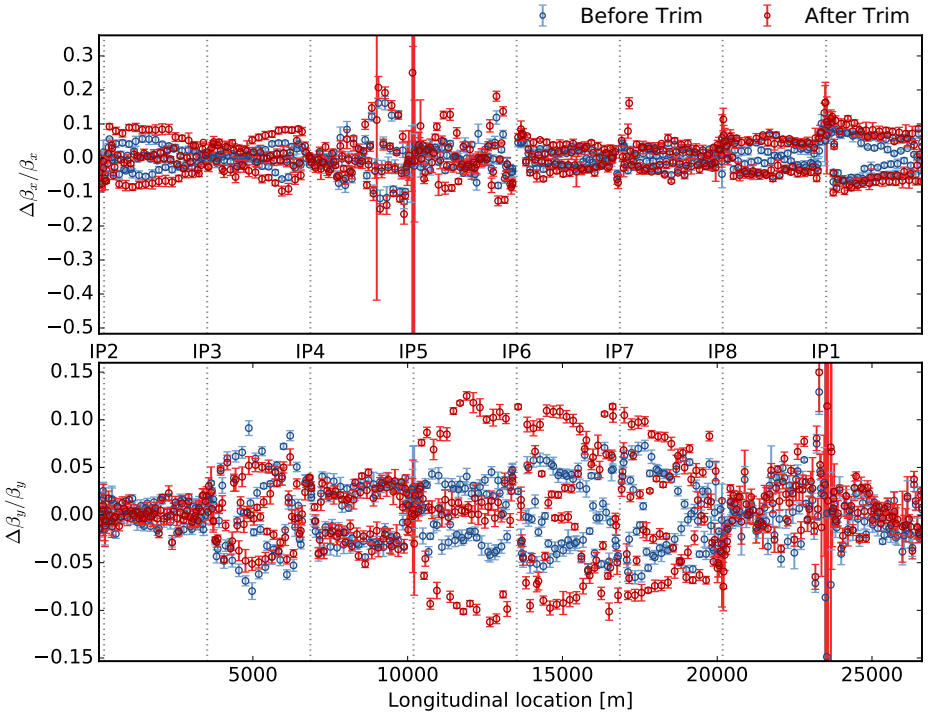

Figure 9: β-beating in Beam 1 before and after waist-correction trim for IP5.

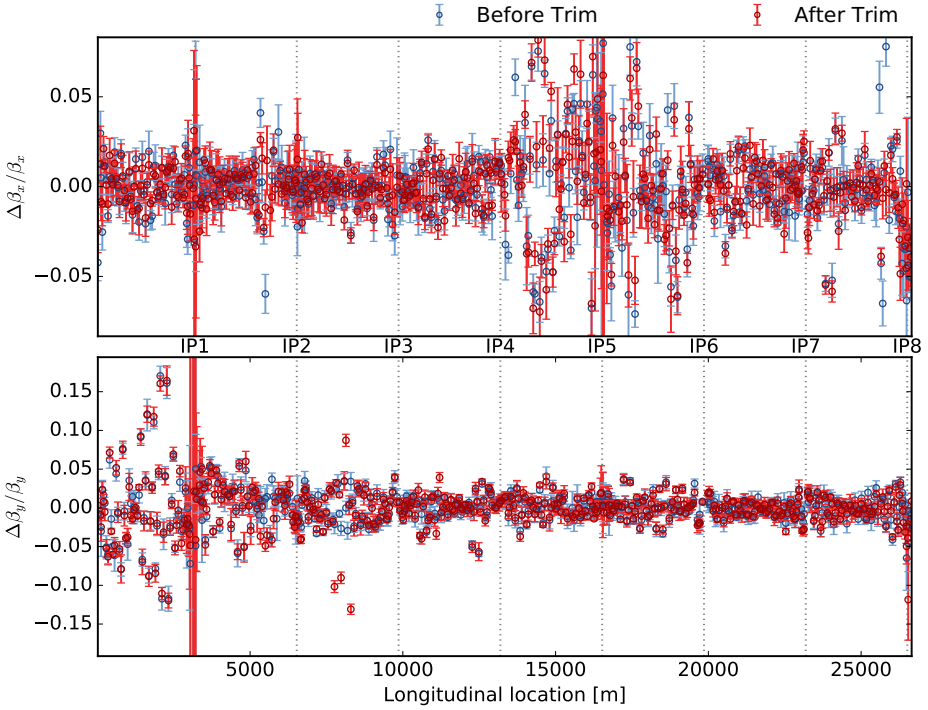

Figure 10: β-beating in Beam 2 before and after waist-correction trim for IP5.

2.2.3 High-Order Field Error Trimming

The MD was split into two parts: First only the expected normal dodecapolar errors (b_6) were trimmed to simulate errors in the HL-LHC. Knob name, trim value and circuit can be found in Table 1. After finishing measurements at this setting, sextupolar and octuplar errors (a_3, b_3, a_4, b_4) were put into the machine on top. Knob names, trims and circuit can be found in Table 2.

The change in beam lifetime, extracted from the Beam Loss Monitors (BLM, Timber: `LHC.BLM.LIFETIME:B[12]_BEAM_LIFETIME`), and in beam intensity, extracted from the Fast Beam Current Transformer (BCTFR, Timber: `LHC.BCTFR.A6R4.B[12]:BEAM_INTENSITY`), are shown in Figs. 11 to 13.

Despite a slight recovery of lifetime after trimming in the b_6 knob, overall there is a lifetime depletion of 25-30% (Fig. 11). While the trim of the b_4 knob does not influence the lifetime at all (Fig. 12), the trimming of the remaining knobs (Fig. 13) leads to a pronounced deterioration of beam lifetime again, which the beams do not fully recover from, leading to a loss in lifetime of 20-25%.

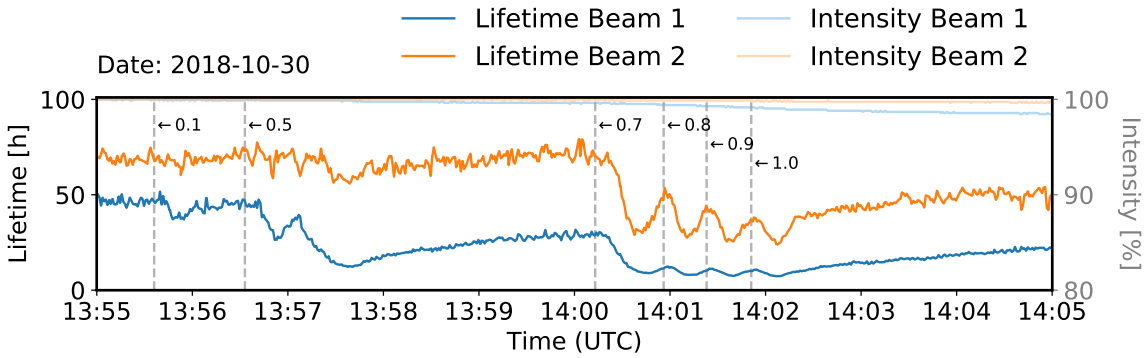

Figure 11: Beam lifetime (from BLMs) and intensity (from BCTFR) during trimming of b_6 knob. The markers show the current trim values.

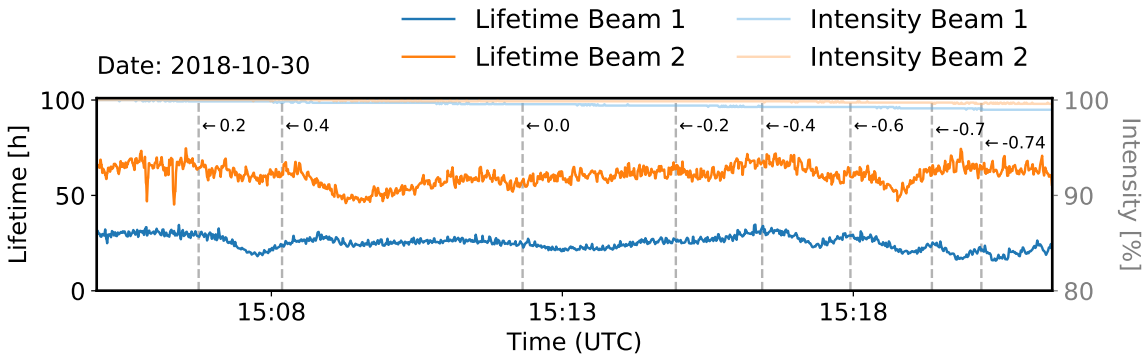

Figure 12: Beam lifetime (from BLMs) and intensity (from BCTFR) during trimming of b_4 knob. The markers show the current trim values.

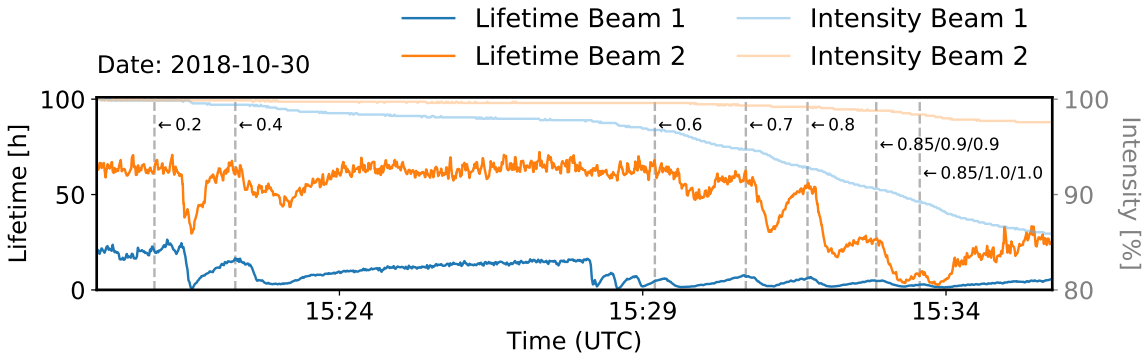

Figure 13: Beam lifetime (from BLMs) and intensity (from BCTFR) during trimming of a_3, b_3 and a_4 knobs. The markers show the current trim values. Multiple values correspond to the $a_3/b_3/a_4$ knobs respectively.

2.2.4 Amplitude Detuning

All amplitude detuning measurements were done using the AC-Dipole (ACD). Its influence on the amplitude detuning direct terms, as described in [25], will need to be corrected for. See [26] for a detailed description of previous amplitude detuning measurements.

The measurements were conducted at two different working points of the AC-Dipole, while keeping the natural tunes constant at the injection tunes, as shown in the tune diagram in Fig. 14.

Beam Lifetime

The measurements were very successful and conclusions could already be drawn from the beam lifetime: At the original AC-Dipole working point at $Q_{x,y}^{ACD} = 0.271, 0.325$, (Working point 1 in Fig. 14) it was possible to kick to peak-to-peak amplitudes useful for analysis of 2.6 mm vertical[1] and 1.6 mm horizontal[2] (at the $\beta = 180$ m BPMs in the arcs). From the recovery of the beam lifetime in Fig. 15, we can see that the losses during these kicks are recovering very slowly, whereas after changing the working point to $Q_{x,y}^{ACD} = 0.275, 0.3$ (working point 2 in Fig. 14) the losses recover fast after the kick. After applying all magnetic field errors expected in the HL-LHC, only vertical kicks could be performed, as the beams were dumped due to triggering the safety measures with an unfortunate kick in Beam 2. Up to then a kick amplitude of only 1.9 mm vertically could be reached, with again only slowly recovering losses. It is not clear what causes the difference between the slow and fast losses in this case, during excited kicks fast losses, only during the excitation period, are the expected behaviour for both hitting a dynamic and a physical aperture, as the beam is brought back to the closed orbit after each kick.

[1] Average from BPMs 20L/21R of IPs 1,3,5,7 and 21L/20R of IPs 2,4,6,8.
[2] Average from BPMs 20L/21R of IPs 2,4,6,8 and 21L/20R of IPs 1,3,5,7.

Detuning

Analysis of the amplitude detuning, similar to [26], has been attempted, yet despite the good kick-amplitudes during the first part of the measurements, the acquired data is very noisy and the natural tune could not be accurately identified in the spectrum. A more detailed analysis with the new software tools [27] or getting the tune of the machine directly from the spectrum of the BBQ-BPM [28, 29] could turn out to be fruitful.

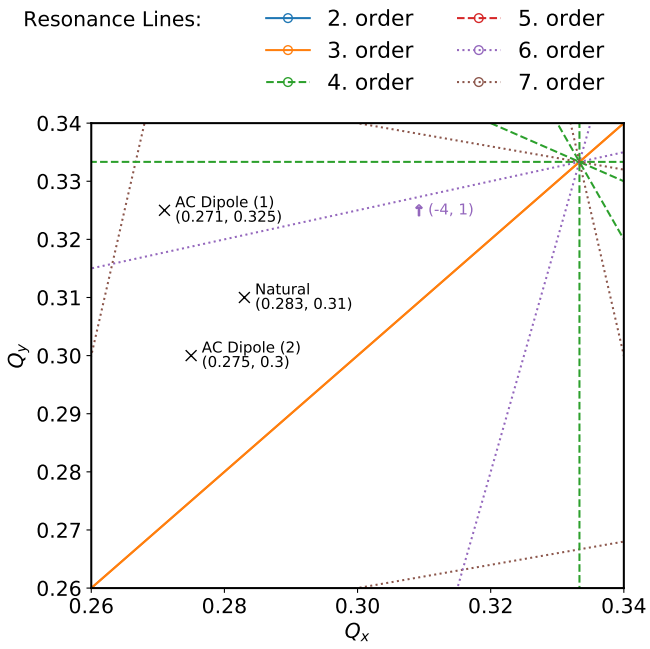

Figure 14: Tune diagram for the working points set during amplitude detuning measurements. The natural tunes were fixed at the injection tunes, while the AC-Dipole tunes were set first to (1), then (2) and back to (1) for the last measurement.

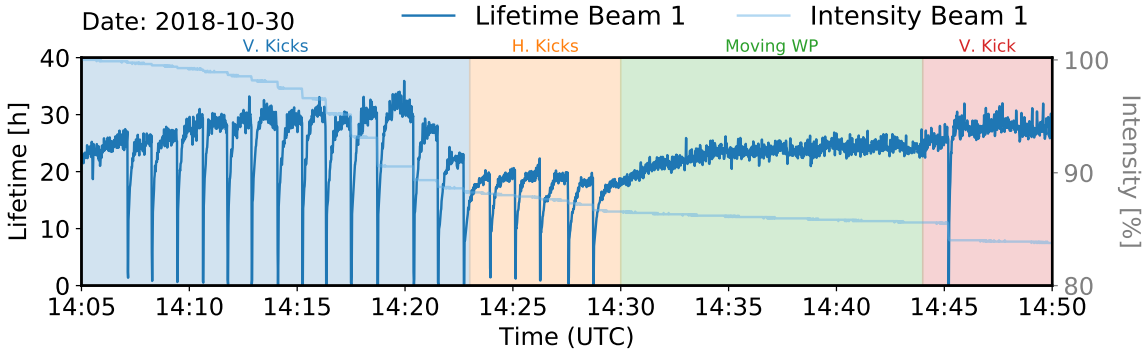

Figure 15: Beam lifetime (from BLMs) and intensity (from BCTFR) during the first part of the kicks for amplitude detuning in Beam 1.

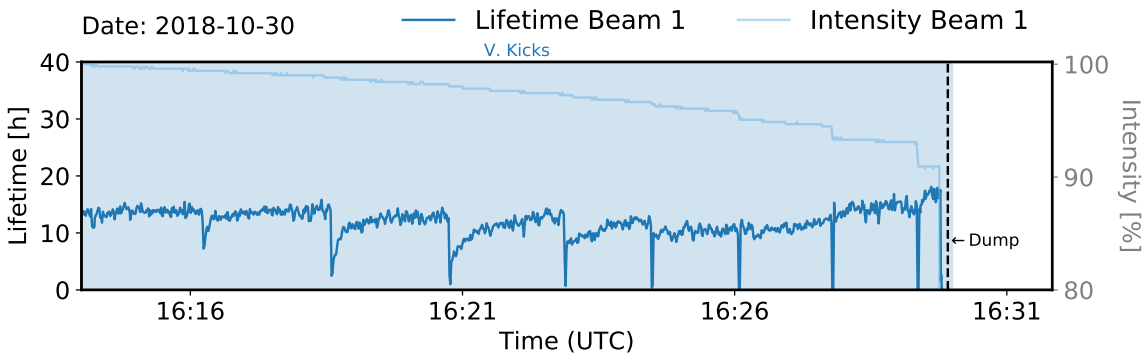

Figure 16: Beam lifetime (from BLMs) and intensity (from BCTFR) during the second part of the kicks for amplitude detuning in Beam 1.

2.2.5 Dynamic Aperture

In Fig. 18 diagonal kicks for measuring DA with b_6 errors applied at the first two working points $Q_{x,y}^{ACD} = 0.272, 0.32$ and $Q_{x,y}^{ACD} = 0.272, 0.30$ show rapid losses and a quick recovery of beam lifetime. While for single kicks this is hinting at hitting a physical aperture, for excited kicks this is the expected behaviour for both, as the beam is brought back to the closed orbit after each kick. On the other hand, the reached maximum peak-to-peak kick amplitudes (at the $\beta = 180\,\mathrm{m}$ BPMs in the arcs) of 1.0 mm and 1.4 mm respectively are below optimum for analysis. At the third working point $Q_{x,y}^{ACD} = 0.292, 0.30$ higher amplitudes of 1.5 mm horizontal and 1.3 mm vertical were reached, and the lifetime recovery was much slower after each kick. With these amplitudes, the data looks more promising for dynamic aperture analysis similar to [16]. Going back to the first working point, the lifetime behaviour from before returned and the maximum kick amplitude went back down to 1.0 mm.

After applying the remaining errors and switching to $Q_{x,y}^{ACD} = 0.292, 0.30$ larger kicks than before could be performed, up to 1.3 mm horizontal and 1.1 mm vertical, which is still less than optimal. Beam lifetime in Fig. 19 shows again rapid recovery after each kick. Back near the original working point, at $Q_{x,y}^{ACD} = 0.266, 0.32$, only a single kick was performed, as 37% of losses were already seen at 2% AC-Dipole strength, which reached a peak-to-peak amplitude of less than 0.9 mm.

The last working point $Q_{x,y}^{ACD} = 0.286, 0.32$ was too close to the dodecapole resonance line (-4, 1) (purple in Fig. 17b) and the beam was dumped due to high losses on the first kick.

Analysis of the data has been attempted, using the forced dynamic aperture algorithm described in [16, 30] and implemented in [31], but due to the quality of the data, no conclusive result could be found so far.

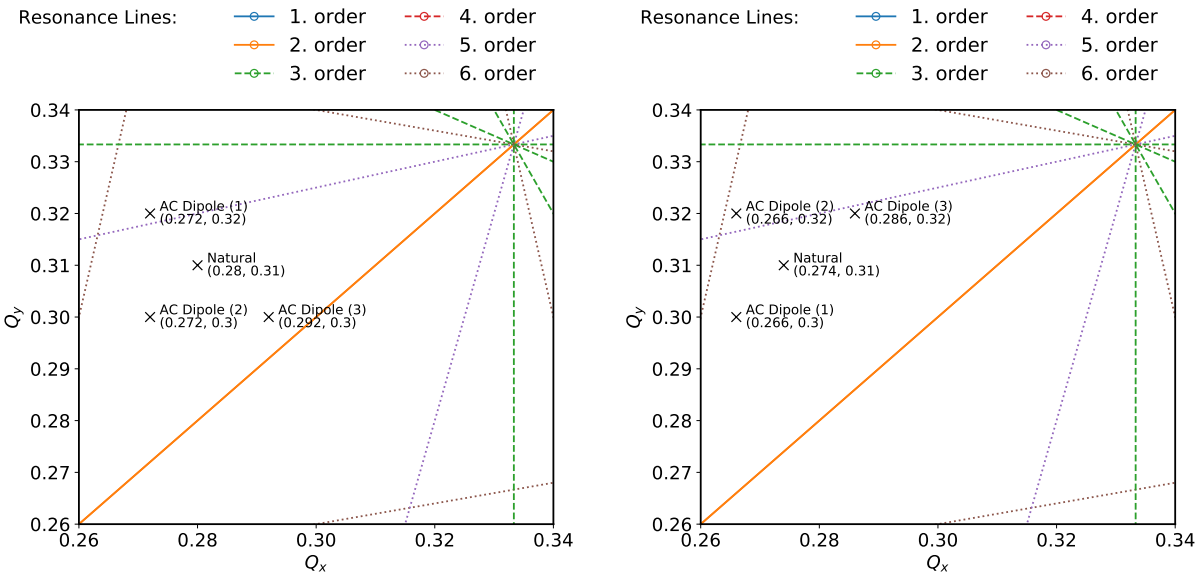

(a) With b_6 (14:10 → 15:05 UTC) **(b)** With a_3, b_3, a_4, b_4, b_6 (16:14 → 16:30 UTC)

Figure 17: Tune diagrams for dynamic aperture measurements.

2.2.6 Resonance Driving Terms

In addition to amplitude detuning and dynamic aperture, the study of resonance driving terms (RDTs) [32, 33, 34] can give valuable insight into the beam stability of the LHC and have been studied in the past [35, 36, 16, 37]. Recent research shows, that measurement and correction of specific RDTs is feasible and leads to improved machine performance [37, 30]. Analysis of the data gathered during this MD is still to be performed and could provide first insights into the RDTs to be expected in the HL-LHC.

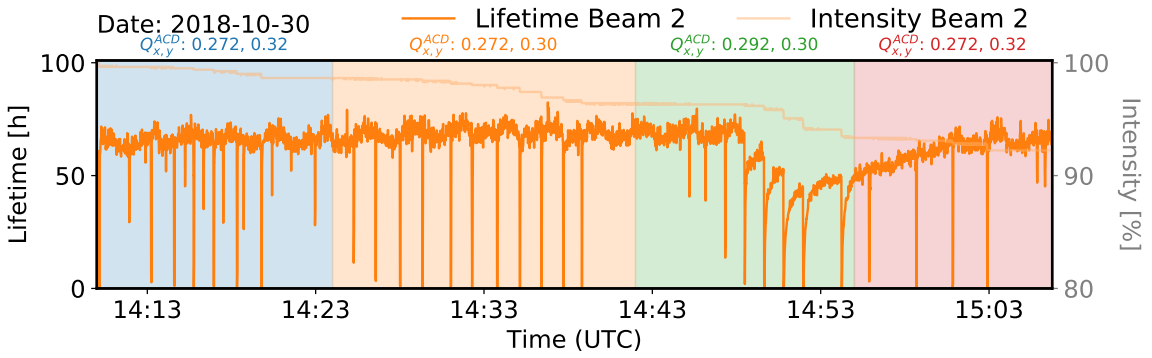

Figure 18: Beam lifetime (from BLMs) and intensity (from BCTFR) during the first part of the kicks for dynamic aperture in Beam 2.

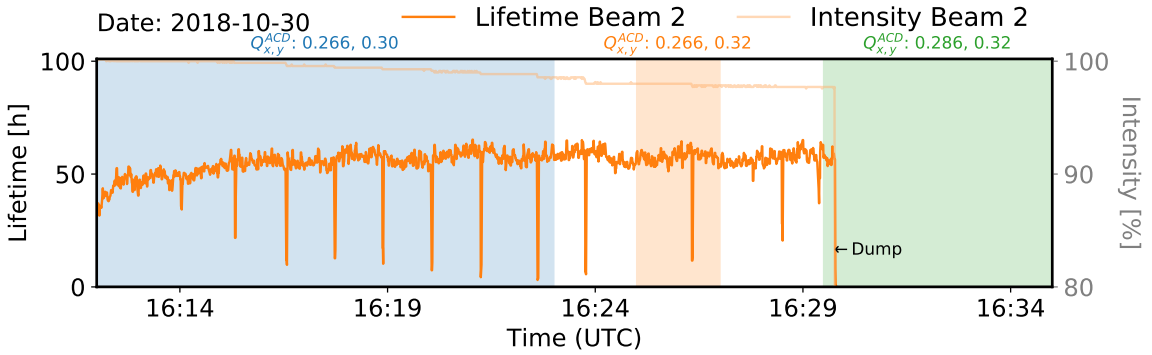

Figure 19: Beam lifetime (from BLMs) and intensity (from BCTFR) during the second part of the kicks for dynamic aperture in Beam 2.

3 Conclusion

MD3312 has been a very demanding, yet fruitful MD and lots of valuable data has been collected to lead the way towards a successful HL-LHC commissioning.

Initial confusion about the increase in β-beating has revealed the strong influence of the tune-feedback when using ATS optics and shows that one has to be cautious when using these sensitive optics.

Another challenge of these advanced optics encountered during the MD was the observed waist-shift in IP5 which was successfully corrected on the fly. A correction crucial for keeping the luminosity high in the HL-LHC.

Further, this MD hints at an expected reduced beam lifetime originating from uncorrected high-order field errors. Analysis of these field errors will be an important part of the HL-LHC commissioning.

The applicability of two measures for non-linear commissioning, dynamic aperture and amplitude detuning, was tested. At first glance amplitude detuning measurements were successful at two working points under test, while dynamic aperture studies proved to be more difficult yet a seemingly working configuration was found. Both measurements are still awaiting a detailed analysis.

The noisiness of the measurement data taken during this MD provides also a valuable insight into the challenges of future commissioning of the HL-LHC: Measurements with high-order nonlinear errors present in the machine will be even more demanding than in the LHC and will require additional preparation and new strategies, to establish consistent methods unperturbed by the presence of these errors.

In the LHC the current strategy for correction is an alternation of linear and nonlinear optics commissioning: linear optics are corrected first at flat-orbit to allow for the nonlinear commissioning to be successful. After correcting sextupole and octupole errors, the linear corrections can be re-optimized to account for the changed optics and improved measurement quality [9]. An adapted scheme might be needed for HL-LHC as well, in which also the current non-linear correction is iterated upon, after correcting high-order errors.

4 Acknowledgements

Many thanks go to the OP and BI groups for the support lent to these studies, especially to the operators present during measurement time, Markus Albert and Matteo Solfaroli Camillocci. A lot of gratitude also to the latter for providing feedback during the planning of the MD. Similarly thanks go to the collimation team for helping facilitate the large amplitude kicks necessary for nonlinear measurements in the LHC. A wholehearted thank you, to the rest of the OMC team, for being always there for answering questions and providing and updating the Beta-Beating software, without which this analysis would not have been possible.

References

[1] E. H. Maclean et al., *Report from LHC MD 2158: IR-nonlinear studies*, Accelerators & Technology Sector Note CERN-ACC-2018-0021, Mar. 2018. URL: https://cds.cern.ch/record/2306295.

[2] R. Tomás, *Adiabaticity of the ramping process of an ac dipole*, Phys. Rev. ST Accel. Beams **8** (2005), p. 024401. doi:10.1103/PhysRevSTAB.8.024401.

[3] R. Tomás, S. Fartoukh and J. Serrano, *Reliable Operation of the AC Dipole in the LHC*, LHC Project Report 1095, 2008. URL: http://cds.cern.ch/record/1122245.

[4] T. Bach et al., *Measurement of amplitude detuning at flat-top and beta*=0.6 m using AC dipoles*, Accelerators & Technology Sector Note CERN-ATS-Note-2013-015 MD, Mar. 2013. URL: https://cds.cern.ch/record/1528610.

[5] R. Tomás, M. Aiba, A. Franchi and U. Iriso, *Review of linear optics measurement and correction for charged particle accelerators*, Phys. Rev. Accel. Beams **20** (2017). doi:10.1103/PhysRevAccelBeams.20.054801.

[6] G. Arduini et al., *High Luminosity LHC: Challenges and plans*, J. Inst. **11** (2016), p. C12081. doi:10.1088/1748-0221/11/12/C12081.

[7] F. S. Carlier et al., *Optics Measurements and Correction Challenges for the HL-LHC*, Accelerators & Technology Sector Note CERN-ACC-2017-0088, 2017. URL: http://cds.cern.ch/record/2290899.

[8] E. H. Maclean et al., *Detailed review of the LHC optics commissioning for the nonlinear era*, Accelerators & Technology Sector Note CERN-ACC-2019-0029, Feb. 2019. URL: http://cds.cern.ch/record/2655741.

[9] E. H. Maclean et al., *New approach to LHC optics commissioning for the nonlinear era*, Phys. Rev. Accel. Beams **22** (2019), p. 061004. doi:10.1103/PhysRevAccelBeams.22.061004.

[10] S. Fartoukh, *Achromatic telescopic squeezing scheme and application to the LHC and its luminosity upgrade*, Phys. Rev. ST Accel. Beams **16** (2013). doi:10.1103/PhysRevSTAB.16.111002.

[11] S. Fartoukh, N. Karastathis, L. Ponce, M. Solfaroli and R. Tomas, *About flat telescopic optics for the future operation of the LHC*, Accelerators & Technology Sector Note CERN-ACC-2018-0018, June 2018. URL: https://cds.cern.ch/record/2622595/.

[12] J. Coello de Portugal et al., *MD2148: Flat optics*, Accelerators & Technology Sector Note CERN-ACC-2018-0051, 2018. URL: https://cds.cern.ch/record/2632141.

[13] J. Coello de Portugal, R. Tomás and M. Hofer, *New local optics measurements and correction techniques for the LHC and its luminosity upgrade*, Phys. Rev. Accel. Beams **23** (2020), p. 041001. doi:10.1103/PhysRevAccelBeams.23.041001.

[14] F. Carlier and R. Tomás, *Accuracy and feasibility of the beta* measurement for LHC and High Luminosity LHC using k modulation*, Phys. Rev. Accel. Beams **20** (2017), p. 011005. doi:10.1103/PhysRevAccelBeams.20.011005.

[15] O. S. Brüning, M. Giovannozzi, S. D. Fartoukh and T. Risselada, *Dynamic aperture studies for the LHC separation dipoles*, Tech. Rep. LHC Project Note 349, CERN, 2004. url: https://cds.cern.ch/record/742967.

[16] F. S. Carlier, R. Tomás, E. H. Maclean and T. H. B. Persson, *First experimental demonstration of forced dynamic aperture measurements with LHC ac dipoles*, Phys. Rev. Accel. Beams **22** (2019), p. 13. doi:10.1103/PhysRevAccelBeams.22.031002.

[17] J. Dilly, E. H. Maclean and R. Tomás, *LHC MD3312: Replicating the HL-LHC DA*, Oct. 2018. url: https://asm.cern.ch/api/files/1456593.

[18] O. S. Brüning and S. D. Fartoukh, *LHC Report 501: Field Quality Specification for the LHC Main Dipole Magnets*, tech. rep., CERN, Oct. 2001. url: https://cds.cern.ch/record/522049.

[19] R. J. Steinhagen, *Real-timefeedback on beam parameters*, Tech. Rep. CERN-AB-2007-008 BI, 2007. url: http://cds.cern.ch/record/1019173/.

[20] B. Auchmann et al., *The magnetic model of the large hadron collider*, Accelerators & Technology Sector Note CERN-ATS-2011-189, CERN, 2011. url: http://cds.cern.ch/record/1281647/.

[21] S. Fartoukh, *An Achromatic Telescopic Squeezing (ATS) Scheme For The LHC Upgrade*, Accelerators & Technology Sector Note CERN-ATS-2011-161, Sept. 2011. url: http://cds.cern.ch/record/1382077.

[22] J. Dilly, R. Tomás and M. S. Camillocci, *Flat-Optics MDs: Observed 5% β-Beating Difference*, LMC Meeting, CERN, Dec. 2018. url: https://indico.cern.ch/event/780656/contributions/3249803/attachments/1769855/2875391/presentation.pdf.

[23] J. Dilly, L. Malina and R. Tomás, *An Updated Global Optics Correction Scheme*, Tech. Rep. CERN-ACC-Note-2018-0056, 2018. url: http://cds.cern.ch/record/2632945.

[24] OMC-Team, *Beta-Beat.src*. CERN. url: https://github.com/pylhc/Beta-Beat.src.

[25] S. White, E. H. Maclean and R. Tomás, *Direct amplitude detuning measurement with ac dipole*, Phys. Rev. ST Accel. Beams **16** (2013), p. 071002. doi:10.1103/PhysRevSTAB.16.071002.

[26] J. Dilly et al., *Report and Analysis from LHC MD 3311: Amplitude detuning at end-of-squeeze*, Accelerators & Technology Sector Note CERN-ACC-NOTE-2019-0042, CERN, Mar. 2019. URL: http://cds.cern.ch/record/2692810/.

[27] OMC-Team et al., *OMC3*. CERN. doi:10.5281/ZENODO.5705625.

[28] M. Gasior and R. Jones, *The Principle and First Results of Betatron Tune Measurement by Direct Diode Detection*, 2005. URL: http://cds.cern.ch/record/883298.

[29] A. Boccardi, M. Gasior, R. Jones, P. Karlsson and R. J. Steinhagen, *First Results from the LHC BBQ Tune and Chromaticity Systems*, 2009. URL: http://cds.cern.ch/record/1156349/.

[30] F. S. Carlier, *A Nonlinear Future: Measurements and Corrections of Nonlinear Beam Dynamics Using Forced Transverse Oscillations*, PhD thesis, Universiteit van Amsterdam, 2020. URL: http://cds.cern.ch/record/2715765/.

[31] OMC-Team, M. Hofer, J. Dilly, F. Soubelet, R. Tomás and T. Persson, *PyLHC*. CERN. doi:10.5281/ZENODO.5643602.

[32] R. Tomás, *Normal form of particle motion under the influence of an ac dipole*, Phys. Rev. ST Accel. Beams **5** (2002), p. 054001. doi:10.1103/PhysRevSTAB.5.054001.

[33] F. Schmidt, R. Tomás and A. Faus-Golfe, *Measurement of Driving Terms*, SPS and LHC Division Note CERN-SL-2001-039-AP, Chicago, 2001. URL: http://cds.cern.ch/record/510665/.

[34] R. Tomás, *Direct Measurement of Resonance Driving Terms in the Super Proton Synchrotron (SPS) of CERN Using Beam Position Monitors*, PhD thesis, Universitat de Valencia, 2003. URL: http://cds.cern.ch/record/615164.

[35] F. S. Carlier and J. Coello de Portugal, *Observations of an Anomalous Octupolar Resonance in the LHC*, in Nonlinear Dyn., 2015, p. 4. URL: https://cds.cern.ch/record/2141782.

[36] F. S. Carlier and J. Coello de Portugal, *Observations of Resonance Driving Terms in the LHC during Runs I and II*, 2016, p. 4. URL: https://cds.cern.ch/record/2141782.

[37] F. S. Carlier, R. Tomás and E. H. Maclean, *Measurement and Correction of Resonance Driving Terms in the LHC*, Submitt. Phys. Rev. Accel. Beams (2020).

Appendices

A Knob Definitions

The knobs used to replicate the conditions in the HL-LHC are given here. In the tables, the names of the circuit and the MAD-X variable are listed, as well as the coefficient used on the current knob-value. Therefore the actual change of the respective magnet strength is given by 'coefficient × knob-value'.

Table 7: Definition of knob *LHCBEAM/2018_MD4_replicatingHL_a3*

Circuit	MAD-X	Coefficient
RCSSX3.L5/K2S	kcssx3.l5	-0.01
RCSSX3.R1/K2S	kcssx3.r1	-0.01
RCSSX3.R5/K2S	kcssx3.r5	0.01
RCSSX3.L1/K2S	kcssx3.l1	0.02

Table 8: Definition of knob *LHCBEAM/2018_MD4_replicatingHL_a4*

Circuit	MAD-X	Coefficient
RCOSX3.R1/K3S	kcosx3.r1	2.5
RCOSX3.L5/K3S	kcosx3.l5	2
RCOSX3.R5/K3S	kcosx3.r5	2

Table 9: Definition of knob *LHCBEAM/2018_MD4_replicatingHL_b3*

Circuit	MAD-X	Coefficient
RCSX3.R5/K2	kcsx3.r5	0.005
RCSX3.R1/K2	kcsx3.r1	-0.003
RCSX3.L5/K2	kcsx3.l5	-0.004
RCSX3.L1/K2	kcsx3.l1	0.006

Table 10: Definition of knob *LHCBEAM/2018_MD4_replicatingHL_b4*

Circuit	MAD-X	Coefficient
RCOX3.L5/K3	kcox3.l5	2
RCOX3.R1/K3	kcox3.r1	2
RCOX3.L1/K3	kcox3.l1	3
RCOX3.R5/K3	kcox3.r5	1.5

Table 11: Definition of knob *LHCBEAM/2018_MD4_replicatingHL_b6*

Circuit	MAD-X	Coefficient
RCTX3.L1/K5	kctx3.l1	30000
RCTX3.R5/K5	kctx3.r5	30000
RCTX3.L5/K5	kctx3.l5	30000
RCTX3.R1/K5	kctx3.r1	30000

Table 12: Definition of knob *LHCBEAM/2018_global_ats_flat_b1_for_ip5_waist* (Part 1)

Circuit	MAD-X	Coefficient
RQ7.L1B1/K1	kq7.l1b1	5.91200296185e-06
RQTL7.L3B1/K1	kqtl7.l3b1	-1.76158877707e-07
RQ9.L2B1/K1	kq9.l2b1	-8.21497792458e-07
RQT12.L4B1/K1	kqt12.l4b1	-1.52063641679e-08
RQ7.R4B1/K1	kq7.r4b1	4.82144059788e-07
RQ9.R2B1/K1	kq9.r2b1	6.26604105491e-07
RQ4.L8B1/K1	kq4.l8b1	5.54536336494e-06
RQ5.R6B1/K1	kq5.r6b1	1.50048963405e-05
RQ7.L4B1/K1	kq7.l4b1	-3.25816387203e-07
RQ4.L5B1/K1	kq4.l5b1	-1.94659951376e-05
RQTL9.R7B1/K1	kqtl9.r7b1	5.50955633116e-07
RQTF.A67B1/K1	kqtf.a67b1	2.48723388552e-08
RQTL7.R3B1/K1	kqtl7.r3b1	1.18945905569e-07
RQ9.L5B1/K1	kq9.l5b1	7.94785194103e-07
RQTF.A34B1/K1	kqtf.a34b1	8.14748357669e-09
RQ10.R6B1/K1	kq10.r6b1	-8.48429135658e-06
RQT13.R2B1/K1	kqt13.r2b1	3.64217811466e-08
RQT13.R5B1/K1	kqt13.r5b1	-6.17687803128e-08
RQT13.L2B1/K1	kqt13.l2b1	-7.53351017124e-08
RQ9.R5B1/K1	kq9.r5b1	-1.16024807539e-06
RQ10.L6B1/K1	kq10.l6b1	-5.25458108314e-06
RQTL11.L8B1/K1	kqtl11.l8b1	3.49561588564e-07
RQTD.A81B1/K1	kqtd.a81b1	-1.43123315866e-06
RQTL11.L3B1/K1	kqtl11.l3b1	-3.87821302184e-07
RQTL11.R3B1/K1	kqtl11.r3b1	1.91673080963e-07
RQ6.R1B1/K1	kq6.r1b1	7.16156364433e-07
RQTD.A56B1/K1	kqtd.a56b1	1.53467226482e-06
RQTL11.R6B1/K1	kqtl11.r6b1	1.68810004197e-06
RQ8.R2B1/K1	kq8.r2b1	6.67564620471e-07
RQ5.L6B1/K1	kq5.l6b1	-2.90860202767e-06
RQT12.R1B1/K1	kqt12.r1b1	1.76833605536e-08
RQT12.L1B1/K1	kqt12.l1b1	3.8105287814e-09
RQT12.R4B1/K1	kqt12.r4b1	-2.75920064574e-09
RQTL11.L5B1/K1	kqtl11.l5b1	-4.81721883716e-07
RQ6.L1B1/K1	kq6.l1b1	-1.85573071576e-06
RQT13.R8B1/K1	kqt13.r8b1	-8.16248586943e-07
RQ8.L2B1/K1	kq8.l2b1	-1.79273982326e-07
RQ6.R4B1/K1	kq6.r4b1	3.71806379462e-07
RQ7.R1B1/K1	kq7.r1b1	-2.23188112614e-06
RQ8.R5B1/K1	kq8.r5b1	2.92720733341e-06
RQ6.L4B1/K1	kq6.l4b1	-2.80306812783e-06
RQT12.R7B1/K1	kqt12.r7b1	3.6425578287e-07
RQ4.R6B1/K1	kq4.r6b1	-1.74905574113e-06
RQT12.L7B1/K1	kqt12.l7b1	1.43910227735e-07
RQ6.R7B1/K1	kq6.r7b1	1.50743053382e-05
RQ8.L5B1/K1	kq8.l5b1	4.90571743228e-08
RQT12.L2B1/K1	kqt12.l2b1	6.59639587397e-09
RQT13.R4B1/K1	kqt13.r4b1	-9.35244912625e-08
RQTL10.R3B1/K1	kqtl10.r3b1	1.05168332709e-07
RQ5.R8B1/K1	kq5.r8b1	-9.81439552561e-06
RQTL8.R7B1/K1	kqtl8.r7b1	-1.88632967024e-07
RQTD.A67B1/K1	kqtd.a67b1	2.21049646143e-07
RQTF.A12B1/K1	kqtf.a12b1	9.28106160814e-08
RQT12.R5B1/K1	kqt12.r5b1	3.80843744097e-07
RQTL10.L7B1/K1	kqtl10.l7b1	4.48761952043e-08
RQTF.A81B1/K1	kqtf.a81b1	-3.07517325382e-07
RQ8.R8B1/K1	kq8.r8b1	1.5592793261e-06
RQ10.L8B1/K1	kq10.l8b1	5.26330813955e-06
RQ7.R2B1/K1	kq7.r2b1	-4.13296447732e-07
RQ10.L1B1/K1	kq10.l1b1	2.98434088108e-07
RQ10.R4B1/K1	kq10.r4b1	-2.32232514463e-06
RQ6.L8B1/K1	kq6.l8b1	-6.33874878986e-06
RQ9.L8B1/K1	kq9.l8b1	1.18571642815e-06
RQT13.L5B1/K1	kqt13.l5b1	6.03183423209e-08
RQ5.R1B1/K1	kq5.r1b1	8.45293243401e-07
RQTL11.R8B1/K1	kqtl11.r8b1	-9.21611274407e-07
RQ4.L2B1/K1	kq4.l2b1	-3.41151817906e-08
RQ8.R1B1/K1	kq8.r1b1	1.33774392452e-07
RQT12.R6B1/K1	kqt12.r6b1	4.56014618067e-07
RQ4.R5B1/K1	kq4.r5b1	3.12492775265e-05
RQ6.L3B1/K1	kq6.l3b1	-1.27883322421e-06
RQTL9.R3B1/K1	kqtl9.r3b1	-2.48518254864e-08
RQT12.L8B1/K1	kqt12.l8b1	-4.23109838721e-07
RQ8.L4B1/K1	kq8.l4b1	4.25050615149e-07
RQTL9.L7B1/K1	kqtl9.l7b1	2.10449934457e-06
RQT13.R3B1/K1	kqt13.r3b1	-3.97924964091e-08
RQ5.R2B1/K1	kq5.r2b1	9.199581541e-07
RQTL11.R1B1/K1	kqtl11.r1b1	-3.67009931779e-07
RQTL8.L3B1/K1	kqtl8.l3b1	2.21115058707e-07
RQ9.R4B1/K1	kq9.r4b1	-1.38918790071e-06

Table 13: Definition of knob *LHCBEAM/2018_global_ats_flat_b1_for_ip5_waist* (Part 2)

Circuit	MAD-X	Coefficient
RQTD.A78B1/K1	kqtd.a78b1	4.07154878701e-08
RQ10.R5B1/K1	kq10.r5b1	2.18877175939e-06
RQ9.L1B1/K1	kq9.l1b1	4.82374616695e-06
RQTL11.L4B1/K1	kqtl11.l4b1	-2.18101988025e-07
RQ10.L2B1/K1	kq10.l2b1	1.72207353444e-06
RQTL11.R7B1/K1	kqtl11.r7b1	-2.93725122447e-07
RQT13.L6B1/K1	kqt13.l6b1	2.055974619e-06
RQ5.L5B1/K1	kq5.l5b1	-1.16574419735e-05
RQ4.L1B1/K1	kq4.l1b1	-4.85875398226e-06
RQTD.A12B1/K1	kqtd.a12b1	4.93974027904e-07
RQ7.L8B1/K1	kq7.l8b1	1.9174915451e-06
RQ6.R5B1/K1	kq6.r5b1	-2.36812684307e-06
RQ6.R2B1/K1	kq6.r2b1	1.71824387962e-06
RQ6.L2B1/K1	kq6.l2b1	1.9265849005e-06
RQ8.R6B1/K1	kq8.r6b1	4.29307328886e-06
RQT12.R3B1/K1	kqt12.r3b1	-3.79768998471e-08
RQ5.L4B1/K1	kq5.l4b1	-4.1329491296e-07
RQT12.L3B1/K1	kqt12.l3b1	1.223027013e-09
RQ8.L6B1/K1	kq8.l6b1	4.4000289563e-06
RQ6.R8B1/K1	kq6.r8b1	6.52010285762e-08
RQ7.R5B1/K1	kq7.r5b1	3.36542289006e-05
RQ10.L4B1/K1	kq10.l4b1	4.98588917708e-07
RQTL7.R7B1/K1	kqtl7.r7b1	9.31328770548e-07
RQ7.L2B1/K1	kq7.l2b1	-4.55098103203e-07
RQ9.R6B1/K1	kq9.r6b1	-4.78668061987e-06
RQ7.L5B1/K1	kq7.l5b1	-2.3855652671e-06
RQ8.L8B1/K1	kq8.l8b1	3.40755696016e-06
RQ7.R8B1/K1	kq7.r8b1	7.91449838289e-06
RQT13.R1B1/K1	kqt13.r1b1	1.13466825269e-07
RQTF.A23B1/K1	kqtf.a23b1	-8.09865330353e-09
RQTL7.L7B1/K1	kqtl7.l7b1	-2.29688566833e-06
RQ9.L6B1/K1	kq9.l6b1	2.22700491577e-05
RQTL11.R2B1/K1	kqtl11.r2b1	-1.31811248139e-07
RQ6.L7B1/K1	kq6.l7b1	-2.04634579859e-05
RQTD.A45B1/K1	kqtd.a45b1	-1.4089361855e-07
RQT13.L1B1/K1	kqt13.l1b1	-5.19084615291e-08
RQTF.A78B1/K1	kqtf.a78b1	7.37936716178e-08
RQTF.A45B1/K1	kqtf.a45b1	-7.82809706834e-07
RQ10.R1B1/K1	kq10.r1b1	1.25471058254e-06
RQ9.L4B1/K1	kq9.l4b1	7.8971442008e-07
RQTL11.L2B1/K1	kqtl11.l2b1	3.27759266838e-07
RQTL11.R5B1/K1	kqtl11.r5b1	9.25595122681e-06
RQTL10.L3B1/K1	kqtl10.l3b1	1.02511137356e-07
RQTL8.L7B1/K1	kqtl8.l7b1	-5.46212447716e-07
RQTL8.R3B1/K1	kqtl8.r3b1	2.8157941756e-07
RQT13.L4B1/K1	kqt13.l4b1	5.68499167741e-08
RQ10.R8B1/K1	kq10.r8b1	-3.69010479062e-07
RQT13.L8B1/K1	kqt13.l8b1	-6.90749857313e-08
RQT13.R7B1/K1	kqt13.r7b1	1.53873088493e-07
RQTL11.L6B1/K1	kqtl11.l6b1	2.16978861545e-08
RQ4.R2B1/K1	kq4.r2b1	-9.29559007545e-07
RQT12.L6B1/K1	kqt12.l6b1	6.69628320793e-07
RQTD.A34B1/K1	kqtd.a34b1	-4.03046342967e-08
RQT12.R8B1/K1	kqt12.r8b1	-1.13879998764e-07
RQ8.L1B1/K1	kq8.l1b1	-1.58218469437e-07
RQ5.R4B1/K1	kq5.r4b1	1.13803866952e-06
RQ5.L1B1/K1	kq5.l1b1	-4.53007487522e-06
RQ6.R3B1/K1	kq6.r3b1	-1.00737452158e-06
RQ9.R1B1/K1	kq9.r1b1	9.60251327342e-07
RQ10.R2B1/K1	kq10.r2b1	-1.43245955542e-07
RQ9.R8B1/K1	kq9.r8b1	-4.02461182603e-06
RQTF.A56B1/K1	kqtf.a56b1	8.12434245745e-06
RQ6.L5B1/K1	kq6.l5b1	-5.45739339941e-06
RQTL10.R7B1/K1	kqtl10.r7b1	-1.4034750393e-06
RQ8.R4B1/K1	kq8.r4b1	-5.36800939699e-07
RQTL11.L1B1/K1	kqtl11.l1b1	3.36496668751e-07
RQ4.R8B1/K1	kq4.r8b1	-4.70769890626e-07
RQTD.A23B1/K1	kqtd.a23b1	-3.5820900024e-08
RQT12.L5B1/K1	kqt12.l5b1	1.80488779478e-08
RQT13.L3B1/K1	kqt13.l3b1	9.41221713902e-08
RQTL11.R4B1/K1	kqtl11.r4b1	2.75736766753e-07
RQ5.L8B1/K1	kq5.l8b1	1.94048470803e-06
RQTL9.L3B1/K1	kqtl9.l3b1	5.76597869895e-07
RQ10.L5B1/K1	kq10.l5b1	-4.60044338979e-06
RQTL11.L7B1/K1	kqtl11.l7b1	6.17918317403e-07
RQT12.R2B1/K1	kqt12.r2b1	9.55550127912e-09
RQ4.R1B1/K1	kq4.r1b1	-7.14080726993e-07
RQT13.R6B1/K1	kqt13.r6b1	-4.6596741754e-07
RQ5.R5B1/K1	kq5.r5b1	1.5552246623e-05